



Predicting Temporal Fluctuations in an Intracellular Signalling Pathway

CARL JASON MORTON-FIRTH AND DENNIS BRAY

Department of Zoology, University of Cambridge, Downing Street, Cambridge CB2 3EJ, U.K.

(Received on 13 August 1997, Accepted in revised form 8 January 1998)

We used a newly developed stochastic-based program to predict the fluctuations in numbers of molecules in a chemotactic signalling pathway of coliform bacteria. Specifically, we examined temporal changes in molecules of CheYp, a cytoplasmic protein known to influence the direction of rotation of the flagellar motor. Signalling molecules in the vicinity of a flagellar motor were represented as individual software objects interacting according to probabilities derived from experimentally-observed concentrations and rate constants. The simulated CheYp molecules were found to undergo random fluctuations in number about an average corresponding to the deterministically calculated concentration. Both the relative amplitude of the fluctuations, as a proportion of the total number of molecules, and their average duration, increased as the simulated volume was reduced. In a simulation corresponding to 10% of the volume of a bacterium, the average duration of fluctuations was found to be 80.7 ms, which is much shorter than the observed alternations between clockwise and counter clockwise rotations of tethered bacteria (typically 2.6 s). Our results are therefore not in agreement with a simple threshold-crossing model for motor switching. However, it is possible to filter the CheYp fluctuations to produce temporal distributions closer to the observed swimming behaviour and we discuss the possible implications for the control of motor rotation.

© 1998 Academic Press Limited

Introduction

Bacteria such as *Escherichia coli* swim by means of helical flagella driven by a rotary motor at their base (reviewed in Parkinson, 1993; Eisenbach, 1996; Stock & Surette, 1996). The motor rotates either counter-clockwise or clockwise—producing smooth swimming “runs” or abruptly-changing “tumbles”, respectively—and switches between the two in stochastic fashion. Control over the duration of runs and tumbles is exerted by a cytoplasmic protein, CheYp, which changes in concentration in response to extracellular stimuli. All of the intracellular proteins in the pathway leading to CheYp have been identified genetically, purified, and sequenced, and many of the enzymatic reactions they catalyse have been analysed kinetically. Mutants lacking identified proteins either singly or in combination have been

isolated in great numbers and their chemotactic responses documented. There is, in short, a uniquely complete set of data, unmatched in any other cell signalling system, on the biochemical circuit controlling this behavioural response.

Several computer models of the reactions in the chemotaxis signal transduction pathway have been developed using deterministic rate equations. These models give a good quantitative account of the average response followed by adaptation of bacteria exposed to attractants and repellents at different concentrations (Goldbeter & Koshland, 1982; Knox *et al.*, 1986; Segel *et al.*, 1986; Hauri & Ross, 1995; Barkai & Leibler, 1997); they also correctly predict the phenotype of more than 40 mutants with deficits in the chemotaxis pathway (Bray *et al.*, 1993; Bray & Bourret, 1995). However, these deterministic models do not easily represent the fine-grained probabilistic

switching of individual flagellar motors, as seen in the rotation of single bacteria tethered to a surface (Block *et al.*, 1982, 1983; Eisenbach, 1990). These fluctuations presumably originate in the performance of individual motors responding to a handful of signalling molecules in their vicinity. A realistic simulation of these events requires the molecules to be represented as individual particles rather than as concentrations, and enzymatic reactions by probabilities rather than as deterministic differential rate equations.

In the present study, we have used a newly developed stochastic program to simulate the temporal fluctuations in CheYp molecules. The size of the fluctuations and their temporal duration are based on experimental values of signalling concentrations and rate constants. We also compared the predicted fluctuations to the distribution of runs and tumbles of a flagellar motor, as observed in bacteria tethered to a surface, and in this way tested threshold-crossing mechanisms for motor switching.

Materials and Methods

The discrete, stochastic simulator described in this paper, called StochSim, employs a simple, novel algorithm in which enzymes and other protein molecules are represented as individual software objects interacting according to probabilities derived from experimentally-observed concentrations and rate constants. Formally, it is a mesoscopic simulator, meaning that it stores an internal representation of every molecule in the system as a unique object, but does not simulate diffusion (Matias, 1995). The program was written in standard C++, according to the ANSI current working paper (Ellis & Stroustrup, 1990), using Microsoft Visual C++ 4.0 and compiled to run on any IBM-compatible PC, using Microsoft Windows 95 or Microsoft Windows NT. The work described in this paper was carried out using a Pentium processor with 16 Mbytes of random access memory. A free copy of the stochastic simulator program can be obtained from the authors upon request or downloaded from <http://aslan.home.ml.org/stochsim.htm>.

When the program is executed, the simulation system is constructed by creating all the necessary objects in turn. First the event manager is created, which is responsible for changing the system during the simulation; for instance, the user may wish to change the concentration of signalling molecules halfway through the simulation. Then the random number generator is created, based on the "ran 1" algorithm which breaks up any sequential patterns

using a shuffle table (Press *et al.*, 1992). Objects representing each type of molecular species in the system are initialised and then large numbers of objects each representing an individual molecule are created. It is possible to create molecules which have specific states, called multi-state molecules; these react according to the state they are in and are usually used to reflect covalent modification, such as protein phosphorylation. A number of dummy, or pseudo-molecules, are also created at this time, which are used in the simulation of unimolecular reactions: if a molecule reacts with a pseudo-molecule, the former may undergo a unimolecular reaction. Next, a look-up table is constructed which defines all the possible ways in which molecules can react in the system. For every bimolecular reaction, the row is selected according to the first reactant and the column by the second reactant; the corresponding entry in the look-up table then gives the probability that these two reactants will react and what the products will be. Finally, objects are constructed that represent variables being output to the screen and saved to file. Each variable is responsible for recalculating its current value as necessary.

Execution follows a very simple algorithm, illustrated in Figs 1 and 2. Time is quantised into a series of discrete, independent time-slices. In each time-slice, one molecule (not a pseudo-molecule) is selected at random. Then, another object, in this case either a molecule or a pseudo-molecule, is selected at random. If two molecules were selected, any reaction that occurs will be bimolecular; if one molecule and a pseudo-molecule were selected, it will be unimolecular. Another random number is then generated and used to see if a reaction occurs. The probability of a reaction is retrieved from the look-up table: if the probability exceeds the random number, the particles do not react; if the probability is less than the random number, the particles react, and the system is updated accordingly. The next time-slice then begins with another pair of molecules being selected. Although it sounds complicated, this process is actually very fast: because each iteration consists of a small number of operations, even a relatively slow Pentium computer can carry out over 200000 iterations every second.

The probabilities that a reaction will occur after the molecules have been selected are calculated as follows (see Appendix A for details):

(1) if the first molecule selected is A and the second is a pseudo-molecule, the probability that A will undergo a unimolecular reaction is:

$$\text{Probability} = \frac{k_1 \times n \times (n + n_0) \times \Delta t}{n_0}$$

(2) if the first molecule selected is A and the second is B, the probability that A will react with B is:

$$\text{Probability} = \frac{k_2 \times n \times (n + n_0) \times \Delta t}{2 \times N_A \times V}$$

where

- n = number of molecules in the system
- n_0 = number of pseudo-molecules in the system
- k_1 = unimolecular rate constant (s^{-1})
- k_2 = bimolecular rate constant ($\text{M}^{-1} \text{s}^{-1}$)
- Δt = time-slice duration (s)
- N_A = Avogadro constant
- V = volume of system (l)

The number of pseudo-molecules is calculated to minimise the stiffness between the unimolecular and bimolecular reactions. For this we require that the probability of the fastest unimolecular reaction is as close to the probability of the fastest bimolecular reaction as possible. Hence, by equating the two probabilities:

$$n_0 = \text{INT} \left(2 \times N_A \times \frac{k_{1,\text{max}}}{k_{2,\text{max}}} \right)$$

where $\text{INT}(x)$ represents the non-zero positive integer nearest to x .

Results

In order to confirm that the stochastic program gives accurate results, it was tested on a number of different enzyme pathways. For example, it was used to examine the kinetic behaviour of the simple linear pathway $A \rightarrow B \rightarrow C$, in which substance A is converted to substance B then substance C via two unimolecular reactions. The results of the stochastic simulation were then compared to the time course of the reaction predicted by the analytical solution of the deterministic rate equations. As shown in Fig. 3, the simulated behaviour of the system, starting with 60 particles of A and averaged over 10 simulations, agrees closely with that predicted by the kinetic equations.

The output of the stochastic program was also compared to that of MIST, a conventional continuous, deterministic simulator (Ehlde & Zacchi, 1995), for a range of more complicated linear and cyclic enzymatic reaction pathways for which analytical solutions were not readily available. The agreement in every case became closer as the number of particles in the simulation increased, and the stochastic program gave precisely the same output when averaged over very large numbers of particles (unpublished results).

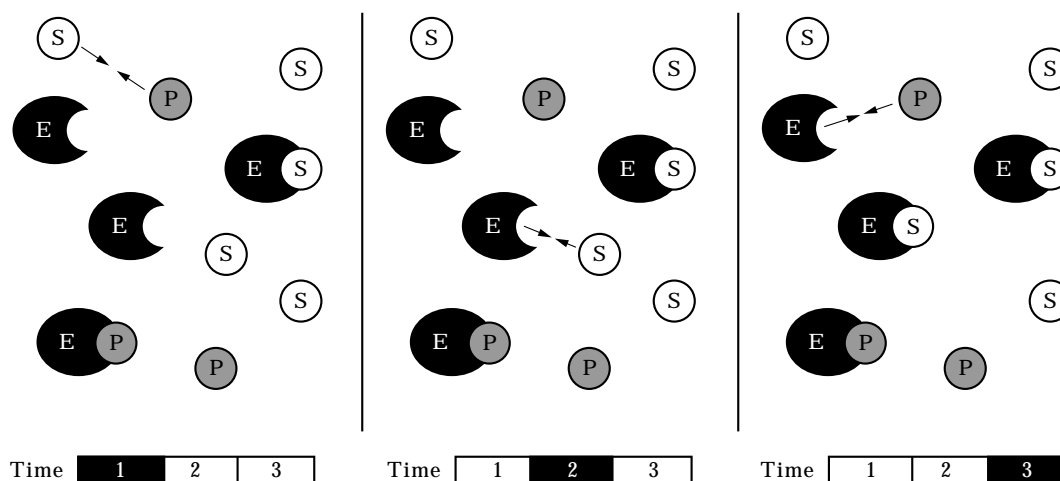


FIG. 1. Series of three slices illustrating the basic algorithm used in this study. Each symbol represents a different molecular object in the program: "E" represents an enzyme, "S" the substrate and "P" the product. The number of these objects is smaller than in a typical simulation. **Left:** In the first time-slice, the computer randomly selects two objects, in this case a substrate and product molecule. When the reaction look-up table is accessed, it indicates that substrate molecules do not react with product molecules; the first time-slice is now complete. **Middle:** An enzyme and substrate molecule are selected in the second-time-slice. Again, the program goes to the reaction look-up table; but this time it finds that the two molecules selected react with a certain probability, p . A random number between 0 and 1 is generated and if it is less than p , as in this example, the reaction does occur. The program updates the system accordingly at the end of the time-slice by binding the substrate to the enzyme to form the enzyme-substrate complex. **Right:** The newly made enzyme-substrate complex is now one of the objects in the simulation and the program continues to select another pair of molecules for reaction.

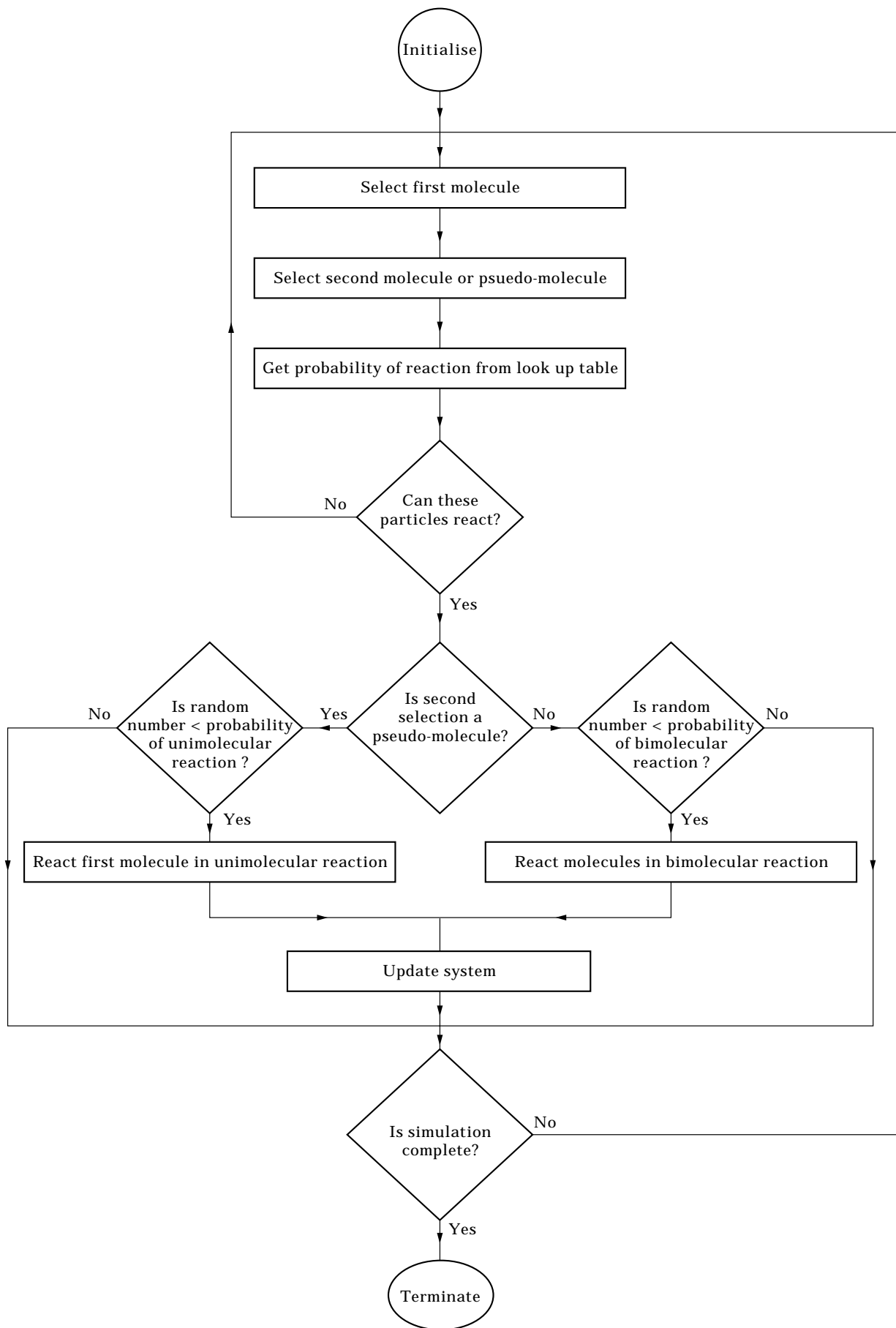


FIG. 2. Flow-chart representation of the stochastic individual-based algorithm.

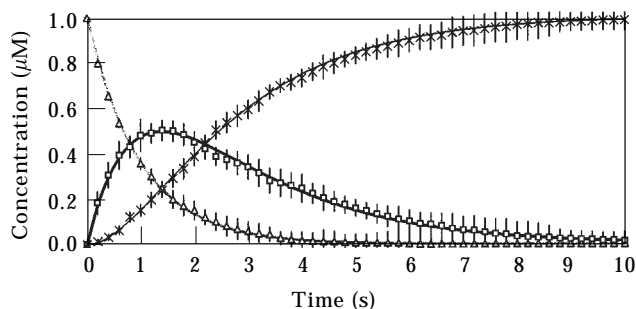


FIG. 3. Comparison between the analytical solution and averaged stochastic simulation (10 simulations with 60 particles each, error bars represent standard deviation) of the simple reaction cascade $A \rightarrow B \rightarrow C$, using a rate of 1.0 s^{-1} for the conversion of A to B and 0.5 s^{-1} for the conversion of B to C. --- [A] (solution); — [B] (solution); — [C] (solution); \triangle [A] (StochSim); \square [B] (StochSim); \times [C] (StochSim).

We then applied the stochastic program to the signalling reactions of bacterial chemotaxis by simulating the reactions of the aspartate response pathway. The aspartate receptor was assumed to be associated on its cytoplasmic domain with the intracellular signalling proteins CheW and CheA, the latter catalysing phosphorylation of CheY. The complex was methylated on four sites by the combined action of CheB and CheR, thereby providing the potential for adaptation. Concentrations and reaction rates were wherever possible taken from the

published literature or, in some cases, from unpublished experimental results. The simulated impulse response of this pathway to attractant matches published experimental data (see Appendix B).

At steady state, all intermediates in the aspartate pathway displayed continual stochastic fluctuations due to the probabilistic nature of the simulation. A typical time course showing changes in numbers of CheYp is shown in Fig. 4. The total number of particles used in this simulation was 2200, which corresponds to approximately the number of chemotactic signalling molecules controlling the rotation of a single flagellar motor (Macnab, 1996). As shown in Fig. 4, numbers of CheYp fluctuated about an average that corresponded precisely to the steady-state concentration obtained by the earlier deterministic computer simulation (Bray & Bourret, 1995). Two parameters used to measure the fluctuations are also indicated on this diagram. The sizes of the fluctuations are measured by their **amplitude**—measured as the difference in numbers of CheYp molecules between the peak of the fluctuation and the mean value. The duration of fluctuations is measured by their **passage time**, defined as the time taken for the number of CheYp molecules to cross the threshold and return.

Both the root mean square amplitude and the mean passage time change with the number of molecules

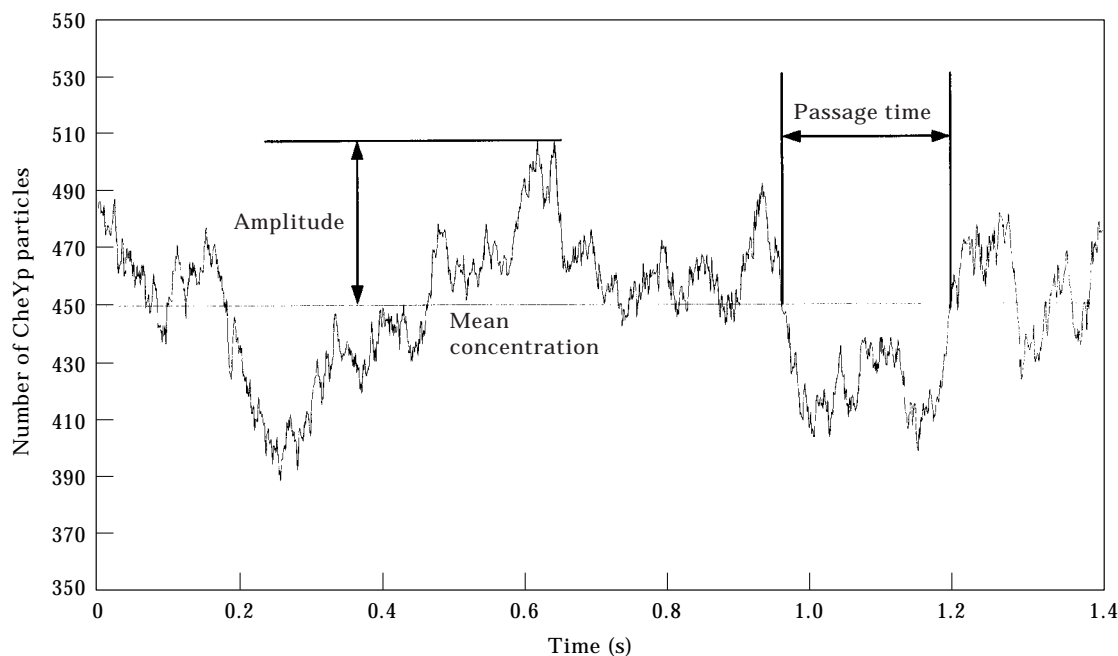


FIG. 4. Fluctuating numbers of molecules of the signalling protein CheYp during a simulation of the reactions of bacterial chemotaxis using the stochastic simulation with 2200 particles. This number of particles corresponds approximately to the number of chemotactic signalling proteins that affect a single flagellar motor. The steady state number of CheYp predicted from a deterministic model (Bray & Bourret, 1995) is also shown. Note that significant deviations from the average occur frequently, even though the system as a whole is at a steady state, and these are characterised by positive and negative passage times, as indicated.

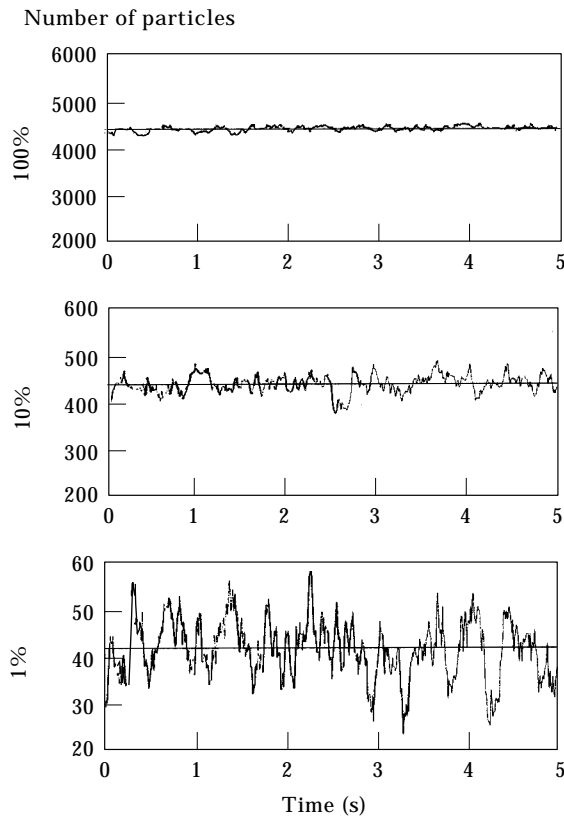


FIG. 5. Variation of fluctuations with the number of particles. CheYp fluctuations are shown for simulations containing 22000, 2200 and 220 particles, corresponding to approximately 100, 10 and 1% of the bacterial volume, respectively. As mentioned in the text, the amplitude of the fluctuations grows as the square root of the number of particles, so that their relative size becomes less as the volume increases. There is also a decrease in the mean passage time as the volume grows larger.

included in the simulation. Figure 5 illustrates sample time courses from simulations of three different sizes, corresponding to 100, 10 and 1% of the total volume of the bacterium. It is immediately apparent from this figure that as the number of molecules increases, the size of their fluctuations relative to the total grows less, corresponding to the fact already mentioned that the simulation approaches the deterministic model as the size of the simulation grows larger. Conversely, when the simulation uses a small number of molecules, the molecular “graininess” of the system becomes apparent, with individual fluctuations corresponding to one or a small number of molecules.

The root mean square amplitude of the fluctuations varies as the square root of the number of particles in the simulation, as expected for a Poisson process [Fig. 6(a)]. The mean passage time also changes according to a simple power function, being largest at very small simulation sizes, and decreasing as the number of particles grows bigger [Fig. 6(b)].

The direction of rotation of the flagellar motor is known to depend on the intracellular concentration of CheYp, with low concentrations producing smooth swimming and high concentrations producing tumbles (Barak & Eisenbach, 1992). It was logical therefore to examine the temporal transitions in CheYp molecules relative to a fixed number of molecules, corresponding to a critical threshold concentration of CheYp, and to compare passage times of positive-going fluctuations with periods of tumbles and passage times of negative fluctuations with periods of runs. In order to make this comparison, the threshold concentration of CheYp was adjusted so that it gave the correct rotational bias (fraction of time spent in smooth swimming runs).

With a threshold value based on a rotational bias of 0.85 (Berg & Brown, 1972) negative-going passage times were found to have an average duration of 80.7 ms. The distribution of these passage times fell on a curve that decreased rapidly with time, approximately matching the sum of two exponential functions (Fig. 7). Positive passage times had a similar distribution but were shifted to the left (not shown). Experimentally determined intervals of runs and tumbles, by contrast, are very much larger than these

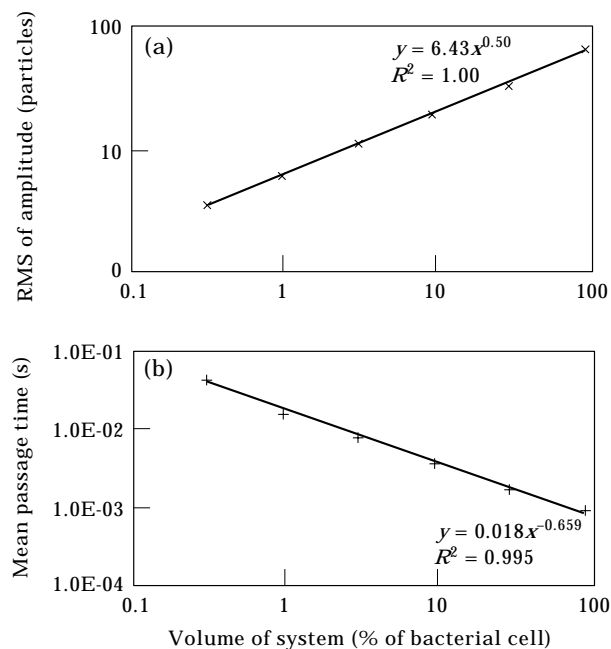


FIG. 6. (a) Distribution of the root mean square of the amplitude of predicted Yp fluctuations for different volumes of the bacterial cell; (b) distribution of the mean passage time of Yp concentration across the mean Yp concentration for different volumes of the bacterial cell.

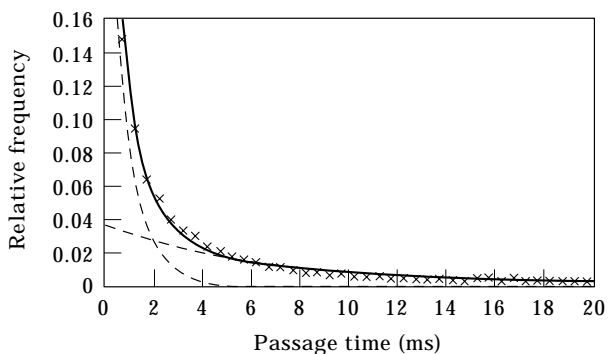


FIG. 7. Distribution of passage times predicted from the Yp fluctuations. The distributions of negative passage times are shown for a number of particles corresponding to 10% of the volume of a bacterial cell. A close fit to the simulated curve may be obtained by summing two exponential curves, as shown here for the positive passage time distribution.

values. Earlier reports gave average values of run duration for tethered bacteria of about 3 s [see, for example, Eisenbach *et al.* (1990)] and we found, in a recent analysis of more than 200 bacteria, an average run length of 2.6 s (manuscript in preparation). The results of our simulation therefore do not support a simple threshold-crossing mechanism for the control of motor switching.

We also examined the possibility that the fluctuations in CheYp could be filtered so as to generate longer intervals that were closer to the periods of runs and tumbles measured experimentally. Filters tried included the following: (i) a running average, in which numbers of CheYp molecules were summed over multiple time points; (ii) a cut-off mask that removed all intervals below a specified duration; (iii) a damping filter, in which changes in CheYp molecules were reduced in proportion to their rate of change; (iv) a two-threshold model in which the switch from a run to a tumble occurs at one Yp concentration, and the switch from a tumble at another Yp concentration (this corresponds to a switch complex in which Yp binding makes the counterclockwise rotation state less stable and the clockwise rotation state more stable). In each case the filtered data was normalised to give the same ratio of runs to tumbles (that is, the same rotational bias) and the distribution of run lengths was examined. Average run lengths of the required duration could be obtained using any of the above filters, and in some cases, they also gave distributions that were similar, although not identical, to the experimental distributions. The two-threshold model (iv) gave the best agreement (Fig. 8).

Discussion

Biochemical reactions are normally studied by analysing their characteristic continuous, deterministic rate equations. Under certain circumstances, however, the deterministic model breaks down and fails to predict the behaviour of the system accurately. Signalling pathways, for example, commonly operate close to points of instability, frequently employing feedback and oscillatory reaction networks that are sensitive to the operation of small numbers of molecules (Hallett, 1989; Goldbeter, 1996). Only 200 K^+ and Na^+ channels responsive to changes in intracellular Ca^{2+} are responsible for a key step in many neutrophil signalling pathways (Hallett, 1989). Gene transcription is controlled by small assemblies of proteins operating in an all-or-none fashion, so that whether a specific protein is expressed or not is, to some extent, a matter of chance (Ko, 1991; Kingston & Green, 1994; Tjian & Maniatis, 1994). The performance of sensory detectors such as retinal rod outer segments (Lamb, 1994; Van Steveninck & Laughlin, 1996) and even the firing of individual nerve cells (Smetters & Zador, 1996) are intrinsically stochastic.

It seems evident that the best way to model such processes on a computer is to use a discrete, stochastic simulator. Stochastic models for the mathematical treatment of enzymatic reactions were first developed in the 1960s and shown to agree “on the average” with the classical deterministic Michaelis-Menten formulation (Bartholomay, 1962). In 1976, Gillespie developed a discrete, stochastic, computational method that was subsequently applied by other groups to analyse biochemical kinetics (Gillespie, 1977, 1979; Hanusse & Blanche, 1981; Stark *et al.*,

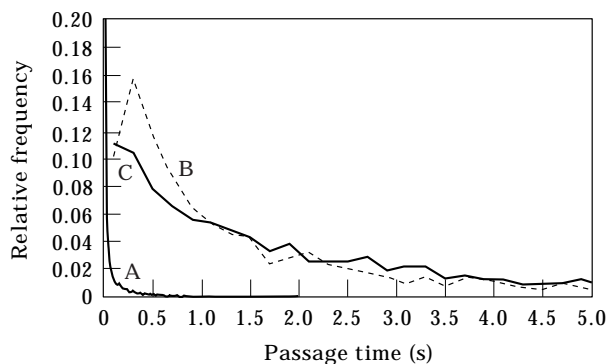


FIG. 8. Distribution of passage times predicted from the Yp fluctuations compared to observed intervals of motor runs and tumbles. (A) The distribution of passage times for a 10% cell volume (from Fig. 5); (B) times obtained with a two-threshold, hysteresis model; (C) experimental values of runs and tumbles intervals.

1993; Breuer & Petruccione, 1995; Matias, 1995). The Gillespie algorithm makes time steps of variable length; in each time step, based on the rate constants and population size of each chemical species, one random number is used to choose which reaction will occur, and another random number, is used to determine how long the step will last (Gillespie, 1976).

The program we describe in this paper differs from the Gillespie algorithm by representing individual molecules rather than individual reactions. It is therefore conceptually simpler and has the advantage that it can readily trace the fate of particular molecules in the course of a series of enzymatic conversions. Our method can also simulate very large numbers of different reactions, such as those produced in cell signalling pathways by the modification of proteins at multiple sites, without becoming impossibly slow. The program has been tested on a wide range of model enzyme systems and shown to generate numbers of individual molecules that vary about a mean corresponding to the macroscopic concentration. The amplitude and duration of these fluctuations are determined by probabilities directly derived from the values of concentrations and rate constants supplied by the user.

In the present study, we used the individual-based, stochastic program to model the signalling reactions of bacterial chemotaxis. We focussed on CheYp molecules because of the key role this species plays in controlling the rotation of the flagellar motor. The average duration and amplitude of the predicted fluctuations in CheYp molecules were found to vary with the number of particles simulated (corresponding to different volumes of the bacterium). The average amplitude varied approximately with the square root of n , the number of particles, as expected for a random based process. The relative size of the fluctuations thus decreased with simulation size (Fig. 5). The duration of fluctuations (measured by the passage time defined in the text) was found to be longest for very small volumes, and to decrease with the number of particles according to an inverse power law ($y \propto n^{-0.659}$).

We also compared the predicted fluctuations in CheYp molecules to the stochastic changes in rotational direction observed experimentally in the rotation of individual flagellar motors. The possibility that motor rotation might be closely coordinated with the instantaneous changes in concentration of an intracellular signalling molecule was first proposed by Koshland (1977). Evidence against this model was presented by Block *et al.* (1983) who showed that it predicted a different distribution of run times to those of individual tethered bacteria, although the differ-

ences between theory and experiment were not large. In our analysis, based on the stochastic simulation we found the average duration of negatively-going excursions in CheYp molecules to be shorter, by several orders of magnitude, than the experimentally-measured run duration. It seems unlikely, given this very large discrepancy, that a simple threshold-crossing model could be responsible for the detailed stochastic fluctuations in rotation of individual motors.

It remains possible that the fluctuations in CheYp molecules might be filtered in some way by the motor. One might imagine, for example, that the motor is unable to switch to a tumble and back again in less than a certain time, or that it requires a certain minimum rate of change of CheYp molecules in order to switch. Although we have not yet explored these possibilities in detail, we did test the effects of a number of algorithmic filters applied to the simulated CheYp fluctuations. We found that all of the filters could give the correct average run and tumble lengths, given appropriate filter parameters. Some were able, in addition, to give distributions of runs and tumbles that corresponded reasonably well to the experimental data (Fig. 8). These and other possibilities could be more easily explored by incorporating a detailed model of the flagellar motor into our simulation and we are currently pursuing this line of enquiry.

The authors wish to thank Matthew Levin and Steven Lay for helpful discussions. This work was funded by Trinity College, Cambridge, and the Medical Research Council.

REFERENCES

- ASAKURA, S. & HONDA, H. (1984). Two-state model for bacterial chemoreceptor proteins. *J. Mol. Biol.* **176**, 349–367.
- BARAK, R. & EISENBACH, M. (1992). Correlation between phosphorylation of the chemotaxis protein CheY and its activity at the flagellar motor. *Biochem.* **31**, 1821–1826.
- BARKAI, N. & LEIBLER, S. (1997). Robustness in simple biochemical networks. *Nature* **387**, 913–917.
- BARTHOLOMAY, A. F. (1962). Enzymatic reaction-rate theory: a stochastic approach. *Ann. N.Y. Acad. Sci.* **96**, 897–912.
- BERG, H. C. & BROWN, D. A. (1972). Chemotaxis in *Escherichia coli* analysed by three-dimensional tracking. *Nature* **239**, 500–504.
- BIEMANN, H. & KOSHLAND, J. E., JR (1994). Aspartate receptors of *Escherichia coli* and *Salmonella typhimurium* bind ligand with negative and half-of-the-sites cooperativity. *Biochem.* **33**, 629–634.
- BLOCK, S. M., SEGALL, J. E. & BERG, H. C. (1982). Impulse responses in bacterial chemotaxis. *Cell* **35**, 215–226.
- BLOCK, S. M., SEGALL, J. E. & BERG, C. B. (1983). Adaptation kinetics in bacterial chemotaxis. *J. Bacteriol.* **154**, 312–323.
- BORCZUK, A., STOCK, A. & STOCK, J. (1987). S-adenosylmethionine may not be essential for signal transduction during bacterial chemotaxis. *J. Bacteriol.* **169**, 3295–3300.

- BORKOVICH, K. A., ALEX, L. A. & SIMON, M. I. (1992). Attenuation of sensory receptor signaling by covalent modification. *Proc. Natl. Acad. Sci. U.S.A.* **89**, 6756–6760.
- BORKOVICH, K. A., KAPLAN, N., HESS, J. F. & SIMON, M. I. (1989). Transmembrane signal transduction in bacterial chemotaxis involves ligand-dependent activation of phosphate group transfer. *Proc. Natl. Acad. Sci. U.S.A.* **86**, 1208–1212.
- BRAY, D. & BOURRET, R. B. (1995). Computer analysis of the binding reactions leading to a transmembrane receptor-linked multiprotein complex involved in bacterial chemotaxis. *Mol. Biol. Cell* **6**, 1367–1380.
- BRAY, D., BOURRET, R. B. & SIMON, M. I. (1993). Computer simulation of the phosphorylation cascade controlling bacterial chemotaxis. *Mol. Biol. Cell* **4**, 469–482.
- BREUER, H. P. & PETRUCCIONE, F. (1995). How to build master equations for complex systems. *Continuum Mech. Thermodyn.* **7**, 439–473.
- EHLDE, M. & ZACCHI, G. (1995). MIST: a user-friendly metabolic simulator. *Comput. Applic. Biosci.* **11**, 201–207.
- EISENBACH, M. (1990). Control of bacterial chemotaxis. *Mol. Microbiol.* **20**, 903–910.
- EISENBACH, M. (1996). Functions of the flagellar modes of rotation in bacterial motility and chemotaxis. *Mol. Microbiol.* **4**, 161–167.
- EISENBACH, M., WOLF, A., WELCH, M., CAPLAN, S. R., LAPIDUS, I. R., MACNAB, R. M., *et al.* (1990). Pausing, switching and speed fluctuation of the bacterial flagellar motor and their relation to motility and chemotaxis. *J. Mol. Biol.* **211**, 551–563.
- ELLIS, M. A. & STROUSTROUP, B. (1990). *The Annotated C++ Reference Manual*. London: Addison-Wesley.
- GILLESPIE, D. T. (1976). A general method for numerically simulating the stochastic time evolution of coupled chemical reactions. *J. Comput. Phys.* **22**, 403–434.
- GILLESPIE, D. T. (1977). Exact stochastic simulation of coupled chemical reactions. *J. Phys. Chem.* **81**, 2340–2361.
- GILLESPIE, D. T. (1979). A pedestrian approach to transitions and fluctuations in simple non-equilibrium chemical systems. *Physica A* **95**, 69–103.
- GOLDBETER, A. (1996). *Biochemical Oscillations and Cellular Rhythms*. Cambridge: Cambridge University Press.
- GOLDBETER, A. & KOSHLAND, D. E., JR (1982). Simple molecular model for sensing and adaptation based on receptor modification with application to bacterial chemotaxis. *J. Mol. Biol.* **161**, 395–416.
- HALLETT, M. B. (1989). The unpredictability of cellular behaviour: trivial or fundamental importance to cell biology. *Perspect. Biol. Med.* **33**, 110–119.
- HANUSSE, P. & BLANCHE, A. (1981). A Monte Carlo method for large reaction-diffusion systems. *J. Chem. Phys.* **74**, 6148–6153.
- HAURI, D. C. & ROSS, J. (1995). A model of excitation and adaptation in bacterial chemotaxis. *Biophys. J.* **68**, 708–722.
- KINGSTON, R. E. & GREEN, M. R. (1994). Modeling eukaryotic transcriptional activation. *Curr. Biol.* **4**, 325–332.
- KNOX, B. E., DEVREOTES, P. N., GOLDBETER, A. & SEGEL, L. A. (1986). A molecular mechanism for sensory adaptation based on ligand-induced receptor modification. *Proc. Natl. Acad. Sci. U.S.A.* **83**, 2345–2349.
- KO, S. H. (1991). A stochastic model for gene induction. *J. theor. Biol.* **153**, 181–194.
- KOSHLAND, D. (1977). A response regulator model in a simple sensory system. *Science* **196**, 1055–1063.
- LAMB, T. D. (1994). Stochastic simulation of activation in the G-protein cascade of phototransduction. *Biophys. J.* **67**, 1439–1454.
- LI, J., SWANSON, R. V., SIMON, M. I. & WEIS, R. M. (1995). The response regulators CheB and CheY exhibit competitive binding to the kinase CheA. *Biochem.* **34**, 14626–14636.
- LUKAT, G. S., LEE B. H., MOTTONEN, J. M., STOCK, A. M. & STOCK, J. B. (1991). Roles of the highly conserved aspartate and lysine residues in the response regulator of bacterial chemotaxis. *J. Biol. Chem.* **266**, 8348–8354.
- LUKAT, G. S., MCCLEARY, W. R., STOCK, A. M. & STOCK, J. B. (1992). Phosphorylation of bacterial response regulator proteins by low molecular weight phospho-donors. *Proc. Natl. Acad. Sci. U.S.A.* **89**, 718–722.
- LUPAS, A. & STOCK, J. B. (1989). Phosphorylation of an N-terminal regulatory domain activates the CheB methylesterase in bacterial chemotaxis. *J. Biol. Chem.* **264**, 17337–17342.
- MACNAB, R. M. (1996). Flagella and motility. In: *Escherichia coli and Salmonella: Cellular and Molecular Biology* (Neidhardt, F. C., ed), pp. 123–145. Washington, D.C.: American Society for Microbiology.
- MADDOCK, J. R. & SHAPIRO, L. (1993). Polar localisation of the chemoreceptor complex in the *Escherichia coli* cell. *Science*, **259**, 1717–1723.
- MATIAS, M. A. (1995). On the effects of molecular fluctuations on models of chemical chaos. *J. Chem. Phys.* **102**, 1597–1606.
- MATSUMURA, P., ROMAN, S., VOLZ, K. & McNALLY, D. (1990). Signalling complexes in bacterial chemotaxis. In: *Biology of the Chemotactic Response* (Armitage, J. P. & Lackie, J. M., eds). Cambridge: Cambridge University Press.
- NINFA, E. G., STOCK, A., MOWBRAY, S. & STOCK, J. B. (1991). Reconstitution of the bacterial chemotaxis signal transduction system from purified components. *J. Biol. Chem.* **266**, 9764–9770.
- PARKINSON, J. S. (1993). Signal transduction schemes of bacteria. *Cell* **73**, 857–871.
- PRESS, W. H., TEUKOLSKY, S. A., VETTERLING, W. T. & FLANNERY, B. P. (1992). *Numerical Recipes in C*. Cambridge: Cambridge University Press.
- SANDERS, D. A. & KOSHLAND, J. E., JR (1988). Receptor interactions through phosphorylation and methylation pathways in bacterial chemotaxis. *Proc. Natl. Acad. Sci. U.S.A.* **85**, 8245–8249.
- SEGALL, J. E., BLOCK, S. M. & BERG, H. C. (1986). Temporal comparisons in bacterial chemotaxis. *Proc. Natl. Acad. Sci. U.S.A.* **83**, 8987–8991.
- SEGEL, L. A., GOLDBETER, A., DEVREOTES, P. N. & KNOW, B. E. (1986). A mechanism for exact sensory adaptation based on receptor modification. *J. theor. Biol.* **120**, 151–179.
- SIMMS, S. A., KEANE, M. G. & STOCK, J. B. (1985). Multiple forms of the CheB methylesterase in bacterial chemosensing. *J. Biol. Chem.* **260**, 10161–10168.
- SIMMS, S. A., STOCK, A. M. & STOCK, J. B. (1987). Purification and characterisation of the S-adenosylmethionine: glutamyl methyltransferase that modifies membrane chemoreceptor proteins in bacteria. *J. Biol. Chem.* **262**, 8537–8543.
- SMETTERS, D. K. & ZADOR, A. (1996). Synaptic transmission—noisy synapses and noisy neurons. *Curr. Biol.* **6**, 1217–1218.
- STARK, S. M., NEUROCK, M. & KLEIN, M. I. (1993). Strategies for modelling kinetic interactions in complex mixtures: Monte Carlo algorithms for MIMD parallel architectures. *Chem. Eng. Sci.* **48**, 4081–4096.
- STEWART, R. C. (1997). Kinetic characterization of phosphotransfer between CheA and CheY in the bacterial chemotaxis signal transduction pathway. *Biochem.* **36**, 2030–2040.
- STOCK, J. B. & KOSHLAND, D. E., JR (1981). Changing reactivity of receptor carboxyl groups during bacterial sensing. *J. Biol. Chem.* **256**, 10826–10833.
- STOCK, J. B. & SURETTE, M. G. (1996). Chemotaxis. In: *Escherichia coli and Salmonella: Cellular and Molecular Biology* (Neidhardt, R. C., ed), pp. 1103–1129. Washington, D.C.: American Society for Microbiology.
- TERWILLIGER, T. C., WANG, J. Y. & KOSHLAND, J. E., JR (1986). Kinetics of receptor modification: the multiply methylated aspartate receptors involved in bacterial chemotaxis. *J. Biol. Chem.* **261**, 10814–10820.
- TIAN, R. & MANIATIS, T. (1994). Transcriptional activation: a complex puzzle with few easy pieces. *Cell* **77**, 5–8.
- VAN STEVENINCK, R. D. R. & LAUGHLIN, S. B. (1996). Light adaptation and reliability in blowfly photoreceptors. *Int. J. Neural Systems* **7**, 437–444.

ZHAO, R., AMSLER, C. D., MATSUMURA, P. & KHAN, S. (1996). FliG and FliM distribution in the *Salmonella typhimurium* cell and flagellar basal bodies. *J. Bacteriol.* **178**, 258–265.

APPENDIX A

Consider a reaction system containing n molecules in a volume, V litres. Suppose it contains n_A molecules of a protein A, which can undergo a simple unimolecular reaction, according to:

$$\frac{d[A]}{dt} = -k_1[A] \quad (\text{A.1})$$

where k_1 is the unimolecular rate constant (s^{-1}).

In a very small time, Δt :

$$\Delta n_A = -k_1 n_A \Delta t \quad (\text{A.2})$$

At time t , we will make two selections: in the first, one molecule will be selected from the reaction system of n molecules; in the second, another molecule will be selected from $n + n_0$ molecules, where n_0 is the number of pseudo-molecules, a non-zero positive integer which is an artificial construct and does not actually represent any molecules. A molecule of protein A will react according to eqn (A.1) with a probability, p_1 , if it is chosen in the first selection and a pseudo-molecule is picked in the second selection; the molecule will not react according to eqn (A.1) in any other way. Therefore, in time Δt , the change in n_A is:

$$\begin{aligned} -\Delta n_A &= \text{Pr}(\text{molecule of A is selected in 1st selection}) \\ &\times \text{Pr}(\text{pseudo-molecule is selected in 2nd selection}) \\ &\times p \end{aligned} \quad (\text{A.3})$$

$$-\Delta n_A = \frac{n_A}{n} \times \frac{n_0}{n + n_0} \times p_1 \quad (\text{A.4})$$

Equating eqns (A.2) and (A.4) gives:

$$p_1 = \frac{k_1 n(n + n_0) \Delta t}{n_0} \quad (\text{A.5})$$

The probability for a bimolecular reaction can be derived similarly. Protein B can react with protein C in a simple bimolecular reaction, according to:

$$\frac{d[B]}{dt} = -k_2[B][C] \quad (\text{A.6})$$

Where k_2 is the bimolecular rate constant ($M^{-1} \text{s}^{-1}$).

In a very small time, Δt :

$$\Delta n_B = -\frac{k_2 n_B n_C \Delta t}{N_A V} \quad (\text{A.7})$$

where N_A is the Avogadro constant.

A molecule of protein B will react with a molecule of protein C according to eqn (A.6) with a probability, p_2 , if either the molecule of B is selected in the first selection and the molecule of C is selected in the second, or vice versa; the molecules will not react according to eqn (A.6) in any other way. Therefore, in time Δt , the change in n_B is:

$$\begin{aligned} -\Delta n_B &= \{ \text{Pr}(\text{molecule of B is selected in 1st selection}) \\ &\times \text{Pr}(\text{molecule of C is selected in 2nd selection}) \\ &\times p_2 \} \\ &+ \{ \text{Pr}(\text{molecule of C is selected in 1st selection}) \\ &\times \text{Pr}(\text{molecule of B is selected in 2nd selection}) \\ &\times p_2 \} \end{aligned} \quad (\text{A.8})$$

$$-\Delta n_B = 2 \times \frac{n_B}{n} \times \frac{n_C}{n + n_0} \times p_2 \quad (\text{A.9})$$

Equating eqns (A.7) and (A.9) gives:

$$p_2 = \frac{k_2 n(n + n_0) \Delta t}{2 N_A V} \quad (\text{A.10})$$

APPENDIX B

Our current model of bacterial chemotaxis is based on the two-state model of chemoreceptor proteins (Asakura & Honda, 1984; Barkai & Leibler, 1997). Each receptor complex consists of two molecules each of Tar, CheW and CheA, and can be in either an active or inactive conformation. The probability that the complex is in an active conformation increases with the number of methyl groups bound, and falls when aspartate is bound (Table B1). If a complex is in the active conformation, CheA can undergo autophosphorylation. The phosphate group can be

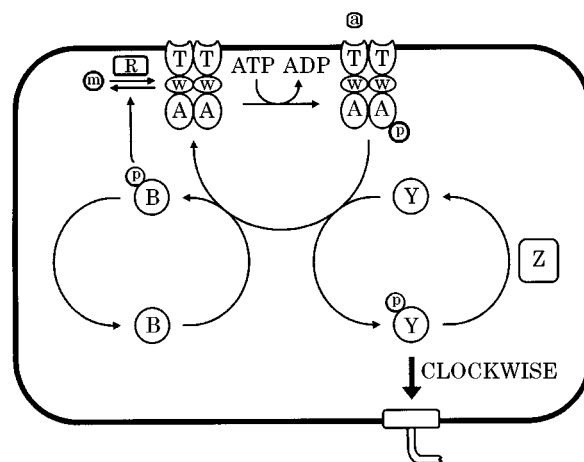


FIG. B1. Simplified diagram of the signal transduction pathway responsible for bacterial chemotaxis.

TABLE B1

Reactions and rate constants used by StochSim in simulations of the chemotaxis pathway

Description	Reaction	k_f	k_r	Notes	
Activation	$E_0 \Leftrightarrow E_0^*$	Pr (active) = 0		The ratio of activity for receptors with 0:2:4 methyl groups is 0:0.489:1.0 (Borkovich <i>et al.</i> , 1992). It is assumed that receptors with 4 methyl groups are always active. The activity of receptors with 1 and 3 methyl groups is estimated by linear interpolation	
	$E_1^* \Leftrightarrow E_1^*$	Pr (active) = 0.246			
	$E_2 \Leftrightarrow E_2^*$	Pr (active) = 0.489			
	$E_3 \Leftrightarrow E_3^*$	Pr (active) = 0.744			
	$E_4 \Leftrightarrow E_4^*$	Pr (active) = 1.0			
		$E_{0a} \Leftrightarrow E_{0a}^*$	Pr (active) = 0		Steady state activity of aspartate bound receptors with 2 methyl groups is 6% that of non-aspartate bound receptors (Borkovich <i>et al.</i> , 1989). The activity of receptors with 1 and 3 methyl groups is estimated by linear interpolation
		$E_{1a} \Leftrightarrow E_{1a}^*$	Pr (active) = 1.48×10^{-2}		
		$E_{2a} \Leftrightarrow E_{2a}^*$	Pr (active) = 2.93×10^{-2}		
		$E_{3a} \Leftrightarrow E_{3a}^*$	Pr (active) = 0.515		
		$E_{4a} \Leftrightarrow E_{4a}^*$	Pr (active) = 1.0		
Demethylation	$E_x^* + Bp \Leftrightarrow E_x^* Bp$	1×10^6	1.25	Bp only binds E in an active conformation (Borcuk <i>et al.</i> , 1987; Sanders & Koshland, 1988). Dissociation constant of E-Bp is $1.25 \mu\text{M}$ (Barkai & Leibler, 1997). Rate of association assumed to be diffusion limited Rate of demethylation by unphosphorylated CheB is $4.28 \times 10^{-3} \text{ s}^{-1}$ (Lupas & Stock, 1989). Increase in activity due to phosphorylation of CheB could be over 100 times higher (R. B. Bourret, pers. comm.; R. C. Stewart, pers. comm.)	
	$E_x Bp \rightarrow E_{x-1} + Bp$	1.3			
Methylation	$E_x + R \rightarrow E_x R$	5×10^6	1.0	R only binds E in an inactive conformation (Terwilliger <i>et al.</i> , 1986; Simms <i>et al.</i> , 1987). The concentration of R is much lower than E (see Table B2) and receptors are localised to the cell pole (Maddock & Shapiro, 1993) suggesting most R is bound to E. Rate of methylation calculated by equating the net rate of demethylation and methylation; in the absence of aspartate, receptors contain 2 methyl groups (Stock & Koshland, 1981; Terwilliger <i>et al.</i> , 1986)	
	$E_x^* R \rightarrow E_{x+1} + R$	15			
Ligand binding	$E + a \Leftrightarrow Ea$	1×10^9	1×10^3	(Biemann & Koshland, 1994)	
Autophosphorylation	$E^* \rightarrow E^*p$	15.5		(R. C. Stewart, pers. comm.)	
CheY reactions	$Y \Leftrightarrow Yp$	1.24×10^{-3}	4.5×10^{-2}	Autophosphorylation and autodephosphorylation (Lukat <i>et al.</i> , 1992; Stewart, 1997) Represents dephosphorylation of Yp by CheZ using bimolecular rate constant of $1.0 \times 10^6 \text{ M}^{-1} \text{ s}^{-1}$ (Lukat <i>et al.</i> , 1991) and CheZ dimer concentration of $14.15 \mu\text{M}$ (Matsumura <i>et al.</i> , 1990)	
		$Yp \rightarrow Y$	14.15		
CheY phosphotransfer	$Ep + Y \rightarrow EpY$	5×10^6		Rate of reaction is limited by the rate of association; transfer of the phosphate group to CheY is much faster than association (Stewart, 1997). Rate of association chosen to be faster than the usual diffusion-limited rate constant of $10^6 \text{ M}^{-1} \text{ s}^{-1}$ due to the speed of the overall phosphotransfer reactions (R. C. Stewart, pers. comm.) Dissociation constant of E-Yp is $4 \mu\text{M}$ (Li <i>et al.</i> , 1995) Dissociation constant of E-Y is $1.5 \mu\text{M}$ (Stewart, 1997)	
		$EpY \Leftrightarrow E + Yp$	20		5×10^6
		$EY \Leftrightarrow E + Y$	7.5		5×10^6
CheB reactions	$Bp \rightarrow B$	0.35		(R. C. Stewart, pers. comm.)	
CheB phosphotransfer	$Ep + B \rightarrow EpB$	5×10^6		Rate of reaction is limited by rate of association; transfer of the phosphate group to CheB is much faster than association (Stewart, 1997). Rate of association chosen to be faster than the usual diffusion-limited rate constant of $10^6 \text{ M}^{-1} \text{ s}^{-1}$ due to the speed of the overall phosphotransfer reactions (R. C. Stewart pers. comm.) Dissociation constant of E-B is $3.2 \mu\text{M}$ (Li <i>et al.</i> , 1995) Dissociation constant assumed to be the same as E-B	
		$EB \Leftrightarrow E + B$	16		5×10^6
		$EpB \Leftrightarrow E + Bp$	16		5×10^6

“E” represents the receptor complex, which can exist in an active (E^*) or inactive (E) conformation; a subscript indicates a particular methylation state (0, 1, 2, 3 or 4). Further information is available on <http://aslan.home.ml.org/expdata.htm>

transferred to CheY, forming CheYp, which binds the motor complex of the flagellum, and increases the probability that it will switch from a counterclockwise to clockwise rotation state (Fig. B1).

The methylation state of the receptor complex is controlled by the methyltransferase CheR and the methyl-er-ase CheB, which add and remove methyl groups, respectively, over a relatively long time scale in such a way as to keep the activity of the receptor complex constant independent of the aspartate concentration. In this way, methylation allows the system to adapt to different concentrations of aspartate. CheR is not controlled directly, but can only bind **inactive** receptor complexes; CheB is activated by phosphotransfer from CheA, and can only bind **active** receptor complexes (Table B1).

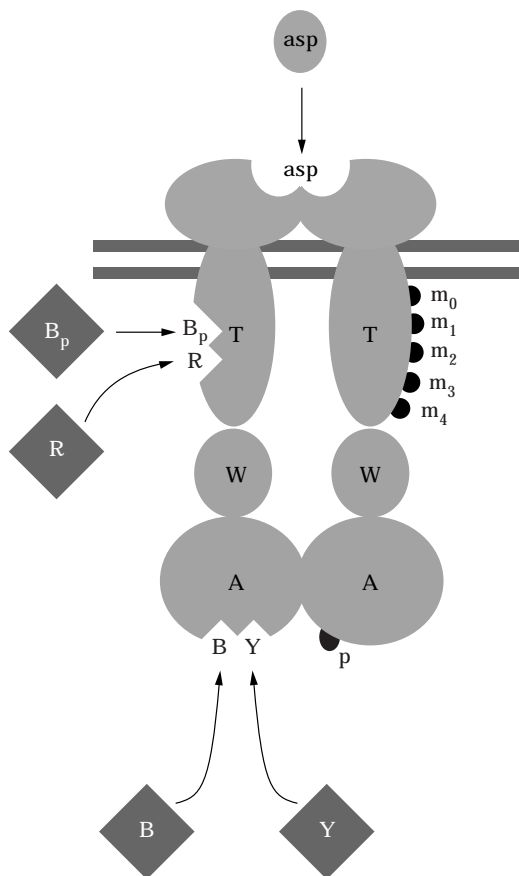


FIG. B2. Illustration of binding sites and methylation states for the chemotaxis receptor complex, which contains two molecules each of Tar, CheW and CheA. Tar dimers can be in one of five methylation states (representing the number of methyl groups), and bind aspartate, phosphorylated CheB and CheR; CheA dimers can be phosphorylated, and bind CheB and CheY; the complex is either in an inactive or active conformation (not shown). This diagram is not meant to represent the actual positions of binding sites on the complex.

TABLE B2
Initial concentrations of chemotaxis proteins used by StochSim

Species	Concentration (μM)	Notes
E(TTWAA)	5	(Ninfa <i>et al.</i> , 1991)
R	0.235	(Simms <i>et al.</i> , 1987)
B	2.27	(Simms <i>et al.</i> , 1985)
Y	18	(Zhao <i>et al.</i> , 1996)

In StochSim, a series of flags are associated with each receptor complex to represent the binding sites and methylation states of the receptor complex (Fig. B2). During a simulation, the exact values of these flags determine how the complex reacts. StochSim was used to simulate the response to an impulse of aspartate using the reactions and rate constants in Table B1 with the initial concentrations in Table B2. The predictions were found to be in agreement with published experimental data (Fig. B3).

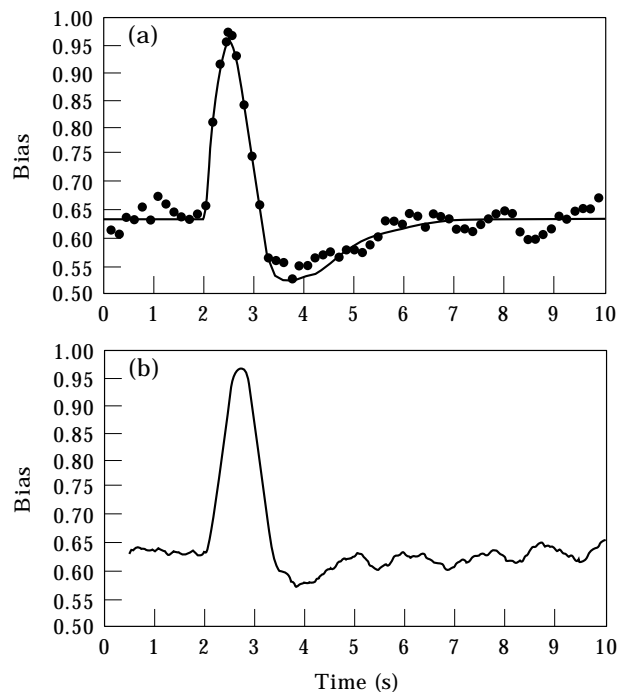


FIG. B3. Impulse response to 1 mM aspartate at 2s: (a) experimental data showing change in bias after release of aspartate by iontophoresis (Segall *et al.*, 1986); (b) Response of signalling pathway predicted by StochSim (bias is calculated from the concentration of Yp using the Hill equation):

$$\text{Bias} = \frac{1}{1 + \frac{3}{7} \left(\frac{[\text{Yp}]}{[\text{Yp}]_0} \right)^{5.5}}$$

where $[\text{Yp}]_0$ is the concentration of Yp in the absence of aspartate).